The influence of snow on sea ice as assessed from simulations of CESM2

Marika M. Holland[1], David Clemens-Sewall[2], Laura Landrum[1], Bonnie Light[3], Donald Perovich[2], Chris Polashenski[2], Madison Smith[3], Melinda Webster[4]

[1]Climate and Global Dynamics Lab, National Center for Atmospheric Research, Boulder, CO, USA
[2]Dartmouth College, Hanover, NH USA
[3]Applied Physics Lab, University of Washington, Seattle, WA, USA
[4]University of Alaska Fairbanks, Fairbanks, AK USA

Correspondence to: Marika M Holland (mholland@ucar.edu)

Abstract. We assess the influence of snow on sea ice in experiments using the Community Earth System Model, version 2 for a pre-industrial and a 2xCO2 climate state. In the pre-industrial climate, we find that increasing simulated snow accumulation on sea ice results in thicker sea ice and a cooler climate in both hemispheres. The sea ice mass budget response differs fundamentally between the two hemispheres. In the Arctic, increasing snow results in a decrease in both sea ice growth and sea ice melt due to the snow's impact on conductive heat transfer and albedo, respectively. This leads to a reduced amplitude in the annual cycle of ice thickness. In the Antarctic, with increasing snow, ice growth increases due to snow-ice formation and is balanced by larger basal ice melt. In the warmer 2xCO2 climate, the Arctic sea ice sensitivity to snow depth is small and reduced relative to that of the pre-industrial climate. Whereas, in the Antarctic, the sensitivity to snow on sea ice in the 2xCO2 climate is qualitatively similar to the sensitivity in the pre-industrial climate. These results underscore the importance of accurately representing snow accumulation on sea ice in coupled earth system models, due to its impact on a number of competing processes and feedbacks.

1 Introduction

Snow is the most reflective natural material on Earth and its presence plays an important role in the cooling of the globe (e.g. Perket et al., 2014). It is also a very effective thermal insulator and thereby reduces the transfer of heat from the underlying surface (e.g. soil or sea ice) into the atmosphere. Its high albedo and its role in heat transfer give it a prominent role in Earth's climate system.

Snow on sea ice is influenced by numerous processes that differ spatially and over time (see Webster et al, 2018 and Sturm and Massom, 2017 for recent reviews). Due to snow optical and thermal properties, it can have competing influences on ice mass budgets that differ by season. During the ice growth season, when sunlight is reduced or nonexistent, the insulating effect

of snow dominates. Although the snow thermal conductivity varies with snow density and metamorphic properties (e.g. Sturm et al., 1997; Sturm et al., 2002; Colonne et al., 2011), field measurements indicate that it is roughly an order of magnitude smaller than that of sea ice. Because of this, a thicker snow cover reduces the amount of heat conducted through the ice pack, resulting in lower surface heat loss to the atmosphere and reduced sea ice growth. In contrast, during the sunlit season, the

35 presence of snow leads to a sizable increase in the surface albedo and less absorption of solar radiation in the snow and ice. This reduces ice melt. The amount of snow on the ice pack can also drive snow-ice formation, which occurs when the weight of the snow submerges the ice-snow interface below the water line, causing seawater to flood the snow and, in freezing conditions, form ice. This ice growth mechanism is significant in the Antarctic (e.g. Maksym and Jeffries, 2000; Massom et al., 2001).

40

Considerable work has elucidated the role of snow in the evolution of the surface albedo of sea ice. As discussed by Perovich et al. (2002), the albedo of Arctic sea ice undergoes a series of phases in its seasonal evolution, in which the presence and state (dry or melting) of snow cover play a central role. When dry snow is present in the spring, the albedo is high (0.8-0.9) and spatially uniform. As melt is initiated, sometimes aided by episodic events such as rainfall on the snow cover, snow grains

45 increase in size leading to a darkening of the surface (to an albedo of around 0.7). With further melt, ponding and bare ice conditions occur, darkening the surface further and contributing to high spatial heterogeneity in surface albedo. In the Antarctic, the ice is mostly snow covered with an absence of ponds, even in summer, and thus the surface albedo remains high and undergoes a much smaller annual cycle than that in the Arctic (e.g. Massom et al., 2001; Brandt et al., 2005).

50 Changes in the timing of Arctic seasonal transitions in a warming climate act to reduce the annual average surface albedo. Satellite data suggest trends of earlier melt onset and a lengthened melt season since 1979 (Stroeve et al., 2014). Satellite observations also indicate reductions in the Arctic surface albedo since the 1980s in part due to reductions in snow on sea ice (Zhang et al., 2019). Climate model simulations (Holland and Landrum, 2015) suggest that changes in the Arctic Ocean surface properties, including an earlier snow melt onset and lengthening snow-free season, remain important for albedo reductions

55 into the future. Additionally, studies indicate that winter ice growth can increase in a warming climate as a direct consequence of the reduced insulating effect of a thinning ice cover with reduced snow (e.g. Bitz and Roe, 2004; Stroeve et al, 2018; Petty et al., 2018).

Models have been used to assess the integrated role of snow and its thermal and optical properties on sea ice and climate

60 conditions. Single-column model studies of Arctic sea ice (Maykut and Untersteiner, 1971; Semtner, 1976), indicate that ice thickness initially decreases with increasing snow depths due to the insulating effect of snow but then increases greatly due to the albedo effect. Under very thick snow conditions, these studies predict a lack of snow-free summers with no surface sea ice melt. A study with a simple energy balance climate model (Ledley 1991) suggested that the overall impact of snow on sea ice is to cool the climate, with the albedo effect of snow dominating. Sensitivity studies in sea ice (e.g., Powell et al., 2005), ice-

65   ocean coupled (e.g. Fichefet and Morales-Marqueda, 1999), and fully coupled (e.g. Blazey et al., 2013) model frameworks indicate that the sea ice mass budgets and other climate characteristics are affected by the snow thermal properties. However, limited work has been done to investigate the overall impacts of changing snow conditions in coupled climate models with active atmospheric feedbacks.

70   Not only does snow on sea ice have a large impact on the climate system, there are multiple reasons why snow accumulation on sea ice may not be accurately represented in models. Significant uncertainties remain in our understanding of the physical processes driving precipitation in the polar regions, resulting in the differences between different reanalysis estimates of snowfall on Arctic sea ice to be of the same order of magnitude as the amount of snowfall (Boisvert et al. 2018). Coupled climate models also exhibit considerable differences in Arctic precipitation (e.g. Kattsov et al., 2007), indicating high structural
75   model uncertainty. Even if the modeled precipitation amounts are accurate, other processes modify the amount of snow on sea ice. Wind-driven blowing snow loss into leads could lead to a 50% reduction in snow on sea ice in the Antarctic (Leonard and Maksym 2011) and is typically not represented in climate models. Finally, sub-grid scale processes could change the impact of snow on sea ice in ways that are analogous to having more or less snow. For example, Sturm et al. (2002) found that accounting for the spatial heterogeneity of snow depth increased the effective thermal conductivity of the snow cover during
80   the SHEBA field campaign by at least 40%.

A better understanding of the influence of snow on sea ice for climate characteristics is important given the large changes underway in the climate system. Indeed, observations suggest that snow on Arctic sea ice is declining in the warming climate in large part because of the later fall ice freeze-up and resulting loss of a sea ice platform to accumulate snow (Webster et al.,
85   2014). Climate simulations project that these changes will continue into the future (Hezel et al., 2012; Webster et al., 2021) with implications for changing albedo and thermal ice growth feedbacks.
Here we address a very basic question: Does changing the amount of snow on sea ice lead to reductions or increases in sea ice area and volume? We use experiments with a coupled climate model in which we impose changes in the amount of snowfall over the sea ice pack, effectively changing the amount of snow on sea ice in both hemispheres. This allows us to isolate the
90   influence of snow on sea ice and determine the net impacts on the sea ice cover and polar climates while accounting for atmospheric feedbacks.

2 Methods

To investigate the role of snow on sea ice, we perform simulations using the Community Earth System Model 2 (CESM2; Danabasoglu et al., 2019). The atmosphere is modeled using the Community Atmosphere Model 6 (CAM6; Gettelman et al.,
95   2019) and land is modeled using the Community Land Model 5 (CLM5; Lawrence et al., 2019). Sea ice is modeled using the CICE sea ice model version 5.1.2 (Hunke et al., 2015). This model includes an elastic-viscous-plastic rheology (Hunke and

Dukowicz, 2002), a sub-grid scale ice thickness distribution (Holland et al., 2006), a multiple-scattering parameterization for solar radiation (Briegleb and Light, 2007) which allows for the inclusion of black carbon and dust aerosols (Holland et al., 2012), and the mushy-layer thermodynamics of Turner and Hunke (2015). More details on the sea ice model and its
100 configuration within CESM2 are available in Bailey et al., (2020).

The CESM2 has a reasonable simulation of Arctic and Antarctic sea ice, including both the mean state and variability (e.g. DeRepentigny et al., 2020; DuVivier et al., 2020; Singh et al., 2020; Raphael et al., 2020). However, simulated Arctic ice is thin compared to observations over the historical period (DuVivier et al., 2020). Simulated snow on Arctic sea ice is also thin
105 compared to observations and accumulates too slowly in the fall (Webster et al., 2021).

For this study, we perform sets of preindustrial and doubled CO2 ($2xCO_2$) simulations with modifications to the amount of snowfall over sea ice. The model uses the full atmosphere, sea ice, and land models of CESM2 but a simplified ocean. In particular, a slab ocean model (SOM) configuration replaces the full depth dynamic ocean model of the standard CESM2. This
110 SOM model configuration has typically been used to assess equilibrium climate sensitivity (e.g. Bacmeister et al., 2020). The SOM computes a single surface ocean mixed layer averaged temperature that evolves subject to time-evolving surface heat fluxes and a prescribed ocean heat flux convergence. The prescribed ocean heat flux convergence is obtained from the fully coupled CESM2 preindustrial control run (Danabasoglu et al., 2020) and accounts for the net dynamic ocean heat flux associated with advection and mixing (Bitz et al., 2012). The use of a SOM configuration allows the system to reach an
115 equilibrated state rapidly (in about 30 years versus hundreds of years for the standard model). Our simulations are run for 50 years and we define the climatology as the average of the last 20 years of simulation after the system has mostly equilibrated. Note that the use of the SOM means that any ocean dynamical feedbacks are excluded although the ocean surface temperature can respond to evolving surface heat fluxes, including changes in shortwave absorption associated with transmission through sea ice and through open water areas.

120

In the standard model, the atmospheric component computes a snowfall amount based on the environmental conditions. In order to modify the snow amount on sea ice, we perform experiments in which the snowfall that the sea ice component receives from the atmosphere is multiplied by a constant factor (Fsnow; Table 1). In doing this, snowfall on sea ice is increased (if Fsnow>1) or decreased (if Fsnow<1) and is gained or lost from the coupled system. We complete simulations with snowfall
125 on sea ice completely removed (Fsnow = 0) to nearly doubled (Fsnow = 1.75). A value of Fsnow=1 is the standard model run in which no change is made to the snow received from the atmosphere model. Note that this method is not conservative in that we are adding or removing snow from the system by altering snowfall as it is received on the ice surface. However, because the changes we impose only affect snowfall over sea ice, they are quite small relative to precipitation on a global mean.

130   Atmospheric feedbacks are active in these experiments and the atmosphere responds to the changing sea ice state. Thus, the exact amount of snowfall is not specified in our experimental design and can vary with the climate. This, along with differences in the fall ice area platform upon which snow can accumulate, result in relative snow volume amounts that vary somewhat from the Fsnow multiplication factor (Table 1). However, the use of the Fsnow factor does effectively modify the amount of snow on sea ice without directly impacting other aspects of the climate system. This allows us to isolate the role of snow on

135   sea ice and assess the net impacts on the sea ice and climate state.

Fsnow value	Annual mean snow volume in the experiments relative to the control (Fsnow=1.0) experiment in the pre-industrial climate	
	NH	SH
0.0	0.00	0.0
0.25	0.21	0.20
0.5	0.46	0.51
0.75	0.72	0.78
1.00	1.00	1.00
1.25	1.27	1.29
1.5	1.66	1.77
1.75	1.94	2.09

Table 1. Experiments and annual mean snow volume in the Northern Hemisphere (NH) and Southern Hemisphere (SH) relative to the control experiment.

3 Results

140   ### 3.1 Control sea ice climate

Some aspects of the sea ice climatology from the control (Fsnow=1.0) simulation are shown in Figure 1. The annual cycle of ice area is compared to present-day observations (Fetterer et al., 2017) in both hemispheres to provide a rough estimate of simulation quality given that observed ice conditions are not available for the preindustrial time period of the model simulations. In the Arctic, the simulated ice area is larger throughout the annual cycle, consistent with the lower greenhouse

145   gas levels present in the simulated preindustrial control climate, and a lack of significant anthropogenic ice loss that has been observed in recent decades. The annual cycle of Antarctic sea ice area agrees very well with present day observations, which is consistent with a much smaller ice loss observed in recent decades in the southern hemisphere. The spatial pattern and mean values of ice thickness are generally consistent with observations or observationally-constrained model simulations (e.g.

Schweiger et al., 2011; Labe et al., 2018; Worby et al., 2008). As observed, the Antarctic ice pack is considerably thinner than
150   that in the Arctic. The monthly maximum in snow thickness occurs in May for the Arctic (consistent with observations, Warren
et al., 1999) and October for the Antarctic. In the Arctic, the simulated May snow is thickest near Fram Strait and thinner
within the shelf regions in general agreement with observations (e.g. Webster et al., 2018). In the Antarctic, the October snow
thickness pattern and magnitudes are reasonable based on the limited observations (e.g. Webster et al., 2018; Kacimi and
Kwok, 2020). The snow thickness pattern closely matches that of the ice thickness which is in part because thicker ice is less
155   prone to snow-ice formation and so can maintain a thicker snowpack.
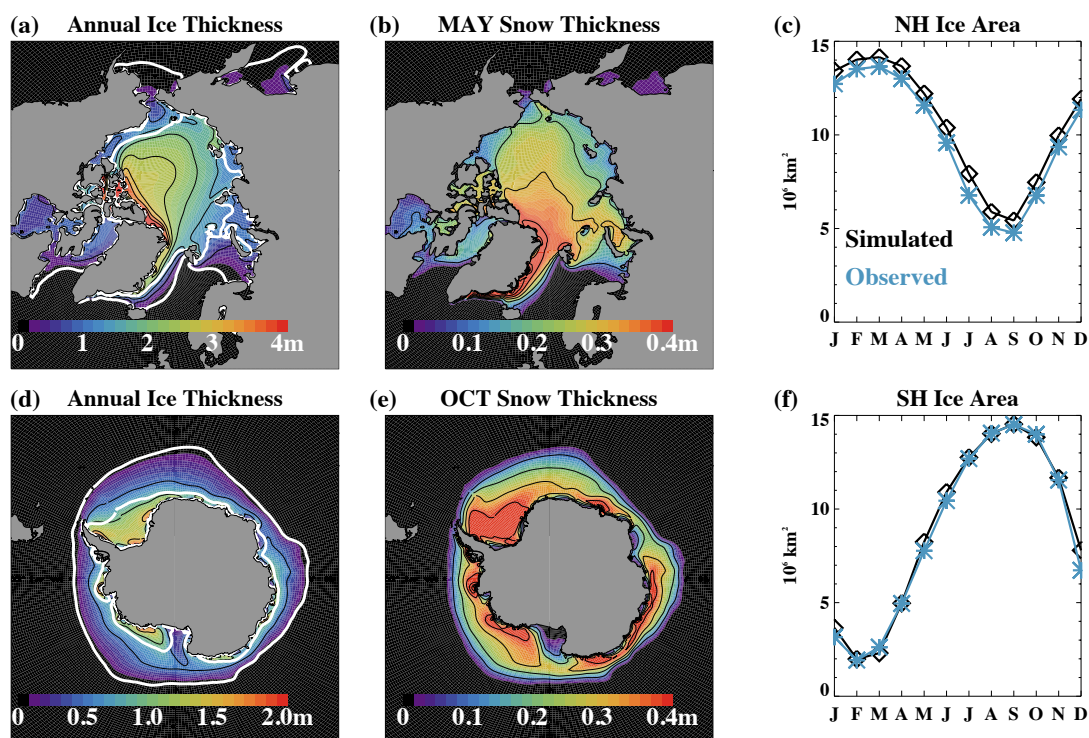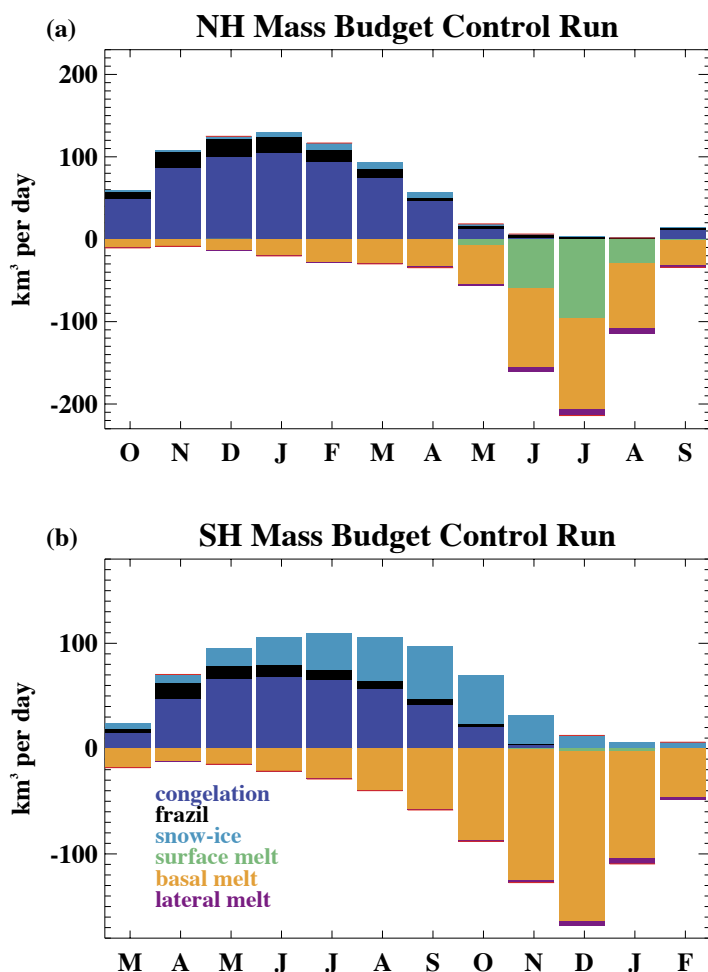

Figure 1. The Northern Hemisphere (a) annual ice thickness, (b) May snow thickness, (c) ice area and Southern Hemisphere
(d) annual ice thickness, (e) October snow thickness, and (f) ice area. Observed ice area averaged from 1979-2013 is from the
160   NSIDC sea ice index (Fetterer et al., 2017). On the maps, the 15% March and September ice concentration contour is shown
in the white contour lines.

The sea ice mass budget that drives the annual cycle is considerably different between the two hemispheres (Figure 2). The
model simulates several distinct ice growth and melt processes. Ice accumulation processes include congelation ice growth
165   onto the base of an existing sea ice pack, frazil ice formation associated with the supercooling of ocean water, and snow-ice

formation. Melting processes are comprised of surface melting at the top of the ice, basal melting at the bottom of the ice, and lateral melting at the sides of floes.

Figure 2. Annual cycle of the climatological ice volume budgets in the Fsnow=1 preindustrial control run for the (a) Northern Hemisphere and (b) Southern Hemisphere. The volume budgets can be directly converted into mass budgets using the constant sea ice density of 917 kg/m3 used in the model. Note that the annual cycle is shifted in both hemispheres to begin with the ice growth season (starting in October for panel (a) and March for panel (b)). Values are computed over the entire hemisphere.

In the Northern Hemisphere (Figure 2a), ice is primarily accumulated through congelation growth from October through April. Frazil ice formation plays a small role. This ice growth is balanced by melting, which occurs year-round with winter basal melt occurring along the ice edge in the north Atlantic and north Pacific. Melt is largest from June through August when the

perennial ice-covered region of the Arctic basin experiences sizable melting at both the surface and the base of the ice. The surface ice melt becomes sizable in June as the snow-free area of the sea ice increases. Other terms in the ice mass budget,
180   including snow-ice formation and lateral melting, make only small contributions to the Arctic mean budgets.

The situation is considerably different for the thinner ice pack of the Southern Hemisphere (Figure 2b). From March through November, ice is accumulated through a combination of congelation ice growth, which dominates at the beginning of the growth season, and snow-ice formation, which dominates at the end of the season. This seasonal transition is in part associated
185   with the region of the ice pack that experiences the majority of growth. This shifts from primarily coastal congelation growth in the early part of the season to snow-ice formation in the thinner, seasonal ice zone later in the season. The substantial snow-ice formation in the Antarctic is associated with the thin ice pack and a snowfall which is over three times greater than that in the Arctic. Frazil ice formation also contributes a small amount of ice mass, particularly in coastal regions (as shown by Singh et al., 2020). Ice melt happens year-round in the Antarctic but is largest from September through February. This melt is almost
190   entirely due to melting at the base of the ice pack. In contrast to the Arctic, surface ice melt is negligible in all months. The differences in basal melting are associated with different oceanography in the two regions, which allows for an annual mean ice-ocean heat exchange in the Antarctic that is about three times larger than that in the Arctic.

These differences between the sea ice mass budgets in the two hemispheres generally agree with observed mass budget
195   information. In particular, the lack of surface melting in the Antarctic is consistent with observations that indicate an ice cover that remains largely snow-covered, even in summer (Massom et al., 2001; Brandt et al., 2005), with few surface melt ponds (Andreas and Ackley, 1982), and heat budget considerations that suggest most Antarctic ice melts from below (Gordon, 1981).

3.2 Influence of different snow thickness on the sea ice and atmosphere state

By adjusting the snowfall received by the sea ice from the atmosphere, we effectively change the hemispheric snow volume
200   and the local snow thickness on the sea ice cover. While we use a constant multiplication factor to make this modification, this does not necessarily result in an equivalent factor change in the hemispheric snow volume as discussed in section 2 (Table 1). This is in part because of the mean ice state changes in the simulations that affect the platform on which snow can accumulate (e.g. Hezel et al., 2012; Webster et al., 2014). Additionally, as discussed further below, atmospheric conditions are responsive to the changing ice climate affecting air temperature and snowfall amounts. While these feedbacks are active in our simulations,
205   our modifications to the model do result in a wide range of snow volume amounts on the sea ice across the different simulations, allowing us to assess the net effect of changing snow amounts on the sea ice state.

Figure 3 shows the mean annual cycle of Northern Hemisphere snow volume, ice volume, and ice area. The differences in the annual mean snow volume across the runs are quite similar to the Fsnow values applied to the snowfall (Table 1), but somewhat
210   larger in the Fsnow=1.5 and Fsnow=1.75 cases. In these high snowfall cases, the annual mean snow volume is 1.66 (for

Fsnow=1.5) and 1.94 (for Fsnow=1.75) times greater than that in the control run. This is associated with larger areas of the Arctic which never reach snow free conditions in summer and high ice concentrations in fall which provide a platform for snow accumulation. The ice volume and ice area generally increase with increasing snow. The simulation with zero snowfall has a fundamentally different climatology with very thin ice and near ice-free conditions in August-October. The high snowfall

215 cases (Fsnow=1.5 and Fsnow=1.75) retain summer snow in the hemispheric values. Although the snow volume annual cycle is larger with higher snow amounts, the amplitude of the ice volume annual cycle declines and ice volume differences across the runs are largest during summer.
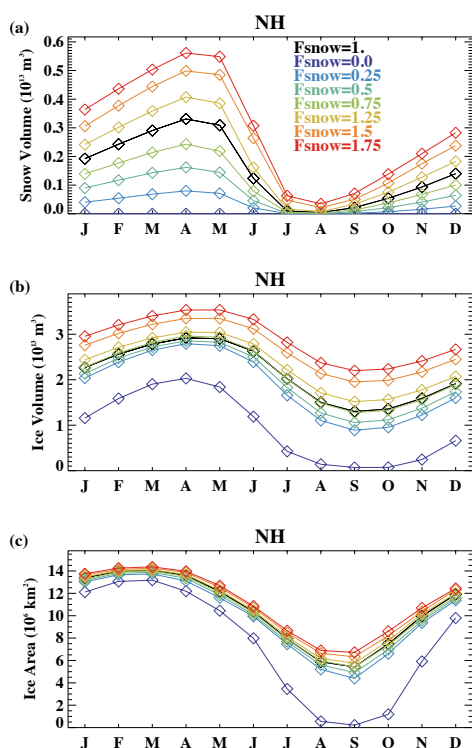
220 **Figure 3**. The Northern Hemisphere (a) snow volume, (b) ice volume and (c) ice area in the different Fsnow experiments.

The nonlinearity of the Northern Hemisphere sea ice response to changing snow thickness is apparent in the summary results shown in Figure 4. The annual mean ice volume and minimum ice area are very low in the case of zero snow thickness. There is a significant jump in ice volume and area for the Fsnow=0.25 case and the annual mean ice volume is then quite similar,

225 ranging from 1.9×10^{13} km^3 to 2.3×10^{13} km^3, for maximum snow volume values ranging from 0.08×10^{13} km^3 to 0.41×10^{13} km^3 (Fsnow from 0.25 to 1.25). However, while the annual mean ice volume is similar across this range of values, the amplitude of the ice volume annual cycle does differ and consistently declines with increasing snow (Figure 4b). This is largely caused by differences in the summer ice volume which appears more sensitive than the winter ice volume amounts for these

intermediate simulations (Figure 3a). The ice area annual cycle also shows a reduction in the amplitude with increasing snow

230 volume, with a large sensitivity in summer and smaller sensitivity in winter (compare the different y-axis range on Figure 4c and 4d). This is consistent with different factors that control the ice edge location in summer versus winter (Bitz et al, 2005) and the strong correlation between ice thickness and summer ice area (Blanchard-Wrigglesworth et al., 2011). The two highest Fsnow runs have maximum Arctic average snow thickness of 0.5 x10^{13} km^3 or greater and exhibit significantly increased ice volume with a reduced annual cycle.

235
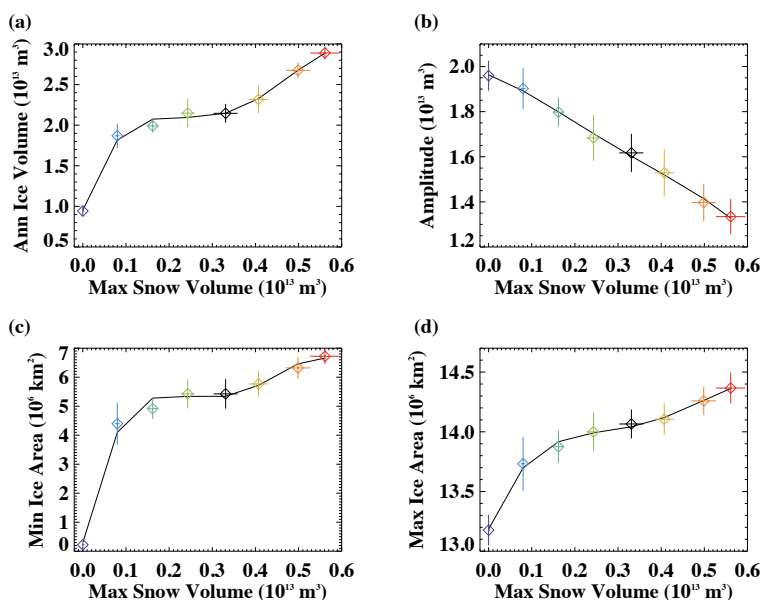
Figure 4. The relationship of the climatological Northern Hemisphere (a) annual ice volume, (b) amplitude of the ice volume annual cycle, (c) annual minimum ice area, and (d) annual maximum ice area versus the annual maximum snow volume. The diamonds show the simulated mean values and whiskers are +/- one standard deviation across the 20 years analyzed for each

240 simulation. The colors the same as in other figures. The black line is a 4th order polynomial fit.

In the Southern Hemisphere (Figure 5), the maximum snow volume is typically larger than that in the Northern Hemisphere. As in the Northern Hemisphere, the Antarctic ice volume and ice area increase with increasing snow volume (Figure 5 and 6) although with a different nonlinear character. The amplitude of the ice volume annual cycle (Figure 6b) increases with snow

245 volume. This is in contrast to the Northern Hemisphere, where a decrease in the ice volume annual cycle amplitude occurs. In the no snow case, ice-free conditions exist for about four months (Figure 5c) and the timing of the maximum ice volume (Figure 5b) occurs a month earlier than in the other simulations.
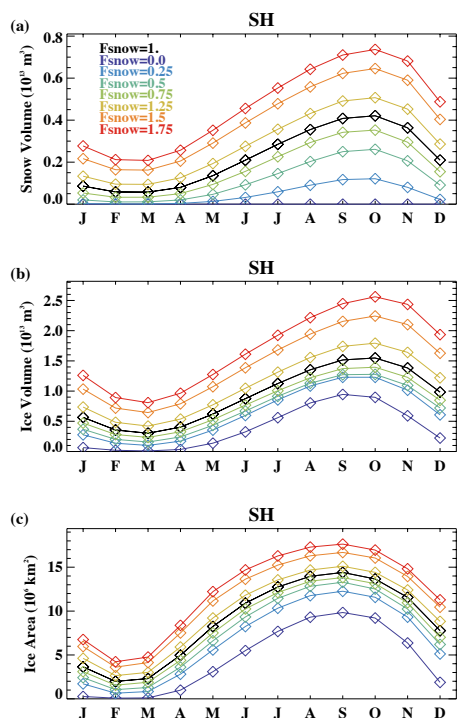
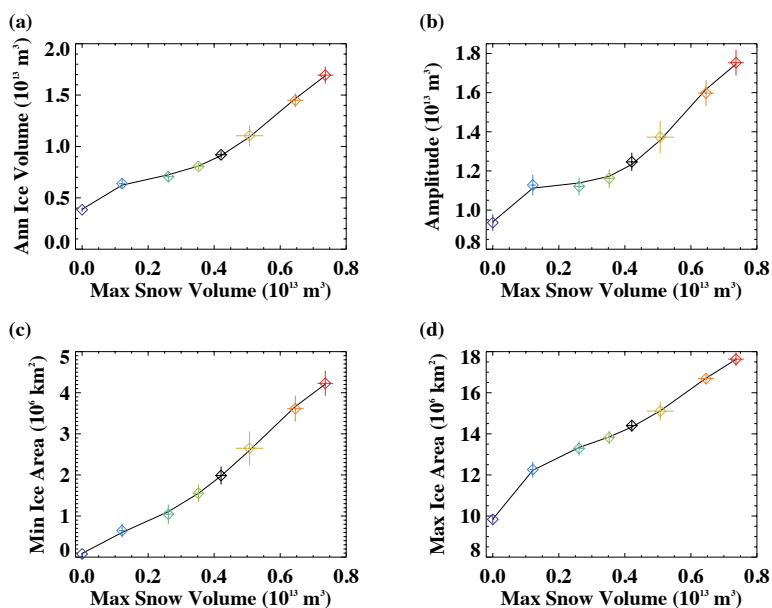**Figure 5.** As in Figure 3 but for the Southern Hemisphere.

Figure 6. As in Figure 4 but for the Southern Hemisphere.

255 The differences in the ice climate associated with changing snow amounts influence and are influenced by changes in the polar atmospheric state (Figure 7). In particular, with increasing snow on sea ice and thicker and more extensive ice in both hemispheres, the atmosphere is colder in both the Arctic and the Antarctic (Figure 7a and 7d). This will feedback and further reinforce the ice state changes. The total high latitude precipitation declines with the colder atmosphere (Figure 7b and 7e), consistent a reduced atmospheric moisture holding capacity and less evaporation from a more ice-covered surface (e.g. Vihma

260 et al., 2015; Bintanja et al., 2014). A greater fraction of this precipitation falls as snow in the colder climates. In the Northern Hemisphere, this somewhat offsets the overall decline in precipitation, resulting in only modest snowfall changes for the 70-90N annual mean across the simulations (Figure 7c). However, in the Antarctic, the relative change in the phase of precipitation is not enough to offset the overall decline and the 70-90S annual mean snowfall is reduced in simulations with increased snow on sea ice (Figure 7f).

265
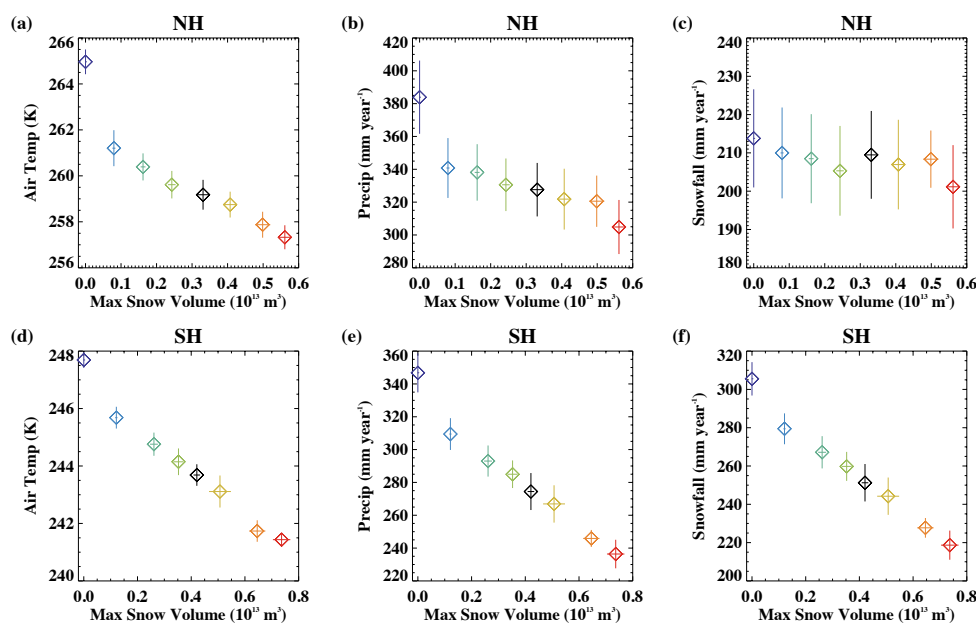
Figure 7. The relationship of the climatological 70-90N (a) annual average surface air temperature, (b) annual total precipitation, (c) annual total snowfall versus the annual maximum Northern Hemisphere volume of snow on sea ice across the simulations. Bottom panels show conditions for 70-90S versus the Southern Hemisphere snow volume for (d) annual mean

270 surface air temperature, (e) annual total precipitation, and (f) annual total snowfall. The whiskers show +/- one standard deviation across the 20 years analyzed for each simulation.

3.3 Differences in the ice mass budgets

Equilibrium sea ice conditions are obtained in the simulations when annual ice melt is basically equivalent to annual ice growth. Figure 8 shows how ice mass budget terms vary with snow volume across the simulations. The two hemispheres show

275 fundamentally different behavior. With increasing snow volume, the total ice growth and melt are relatively insensitive in the
Northern Hemisphere but increase considerably in the Southern Hemisphere. In the Southern Hemisphere, this is consistent
with an increase in the ice volume annual cycle (Figure 6b). However, in the Northern Hemisphere, the relative insensitivity
of the total ice growth or ice melt to changing snow conditions appears to contradict the reduction in the ice volume annual
cycle with increasing snow volume (Figure 4b). This occurs because, on the hemispheric scale considered here, ice melt and
280 growth happen throughout the year and so changes in the magnitude of these terms are not necessarily associated with seasonal
ice loss and gain.
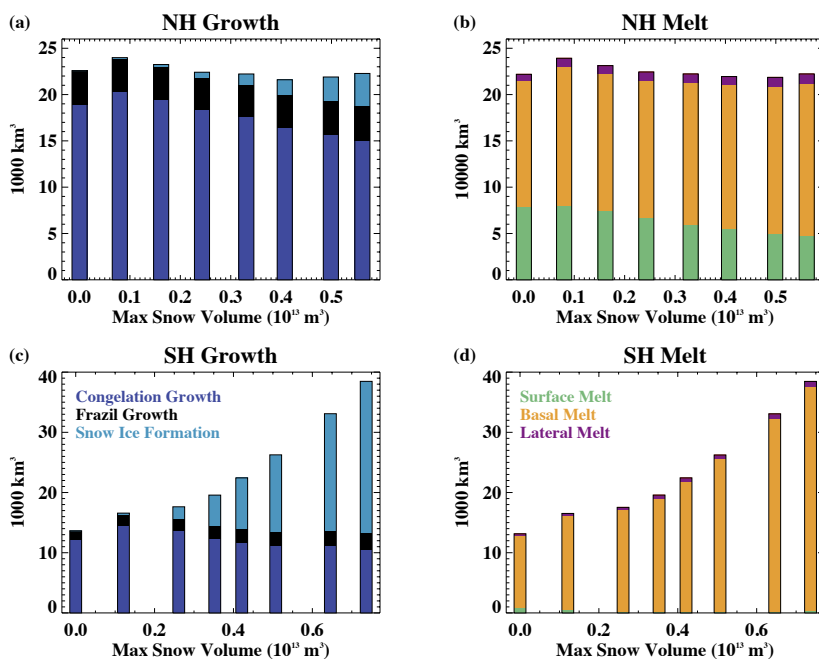
Figure 8. The volume of total annual (a) Northern Hemisphere ice growth, (b) Northern Hemisphere ice melt, (c) Southern
285 Hemisphere ice growth, and (d) Southern Hemisphere ice melt as a function of the maximum snow volume across the
simulations.

In both hemispheres, the congelation ice growth declines with greater snow volumes (Figure 8a and 8c), consistent with a
greater insulating effect of the snow. This occurs in spite of lower air temperatures in the simulations with more snow (Figure
290 7a and 7d), which are themselves partly a consequence of reduced heat conduction and hence lower surface heat loss to the
atmosphere. With thicker snow, the snow-ice formation increases in both hemispheres. Frazil ice formation remains quite
similar across the runs. The dominance of these different ice growth changes differs considerably in the two hemispheres. In
the Northern Hemisphere, changes in the ice mass budgets are quite small and there is a rough balance between the decrease
in congelation ice growth and increase in snow-ice formation. This leads to a weak sensitivity in total ice growth. However, in

13

295   the Southern Hemisphere, the snow-ice formation changes are very large. They overwhelm the decreasing congelation growth, leading to a net increase in ice growth with increasing snow volume.

The simulations performed here reach an equilibrated state and thus the changes in ice growth are balanced by changes in ice melt. In the Northern Hemisphere (Figure 8b), there are reductions in the total surface ice melt with increasing snow volume.

300   This is related to a later transition to a snow free surface in the summer, a shorter snow free season, and higher surface albedo. The total hemispheric basal ice melt generally increases with increased snow volume which is largely a consequence of the greater ice area and larger seasonal ice cover that is present. Notably, for the simulations with maximum hemispheric snow volume greater than 0.5×10^{13} m^3 (the Fsnow=1.5 and Fsnow=1.75 cases), a large fraction (about 50%) of the summer Arctic sea ice remains snow covered with that ice experiencing no surface melt. The perennial snow cover in these simulations results

305   in a consequently larger sensitivity of the total hemispheric ice volume to snow volume as seen in Figure 4a.

In the Southern Hemisphere (Figure 8d), lateral and surface melt are low across all simulations. Surprisingly, even with no snow on sea ice, the surface melt is only 7% of the total annual melt. In the Antarctic, much of the ice forms in coastal regions and is transported away from the continent, where it subsequently melts from its base due to large ice-ocean heat exchange.

310   This allows basal ice melt to occur year-round (Figure 2b) and this term dominates even when no snow cover is present to protect the ice surface from melting. With increasing snow depth, the basal ice melt increases. This is not a direct response to the changing snow conditions, but instead results from the mostly seasonal Antarctic ice and the larger volume of ice available to melt in the thicker snow cover simulations.

315   In order to better understand the differences in the sensitivity to snow cover across the Northern and Southern Hemispheres, it is illustrative to consider the average mass budgets in the perennial and seasonal ice packs separately (Figure 9 and 10). Here we define the perennial ice pack region as the area that has greater than 0.15 ice concentration at the annual ice area minimum, which occurs in September in the Northern Hemisphere and February in the Southern Hemisphere. The seasonal ice pack encompasses the region where ice is present at greater than 0.15 ice concentration at the time of the annual ice maximum

320   (March for the Northern Hemisphere and September for the Southern Hemisphere) but excluding the perennial ice region. The ice growth and melt budgets do not balance within these regional domains because ice can be transported between them. For perennial ice (Figure 9a), congelation growth declines considerably and non-linearly with increasing snow depths. This dominates the net growth sensitivity for Northern Hemisphere perennial ice. This is balanced by ice melt that also decreases with increasing snow depths (Figure 9b). The reduced ice melt at both the surface and base of the ice is consistent with the

325   higher surface albedo which reduces shortwave absorption within both the sea ice and ocean.
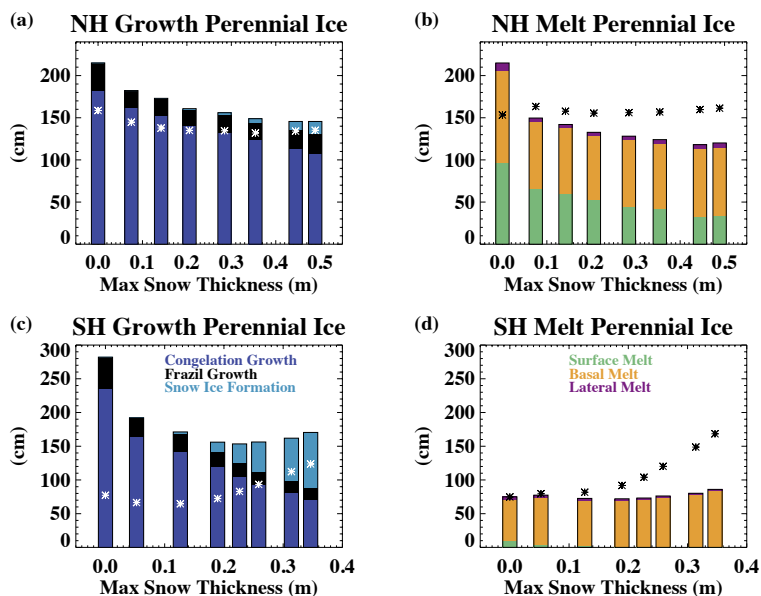
Figure 9. The perennial sea ice average (a) Northern Hemisphere ice growth, (b) Northern Hemisphere ice melt, (c) Southern Hemisphere ice growth, and (d) Southern Hemisphere ice melt as a function of the maximum perennial ice-zone snow thickness across the simulations. The asterisks show the net ice growth and melt for the seasonal sea ice domain for comparison (shown

330 in more detail in Figure 10). Note that the imbalance between the net ice growth and melt in an individual experiment results from ice motion that transports ice between the perennial and seasonal sea ice zones.
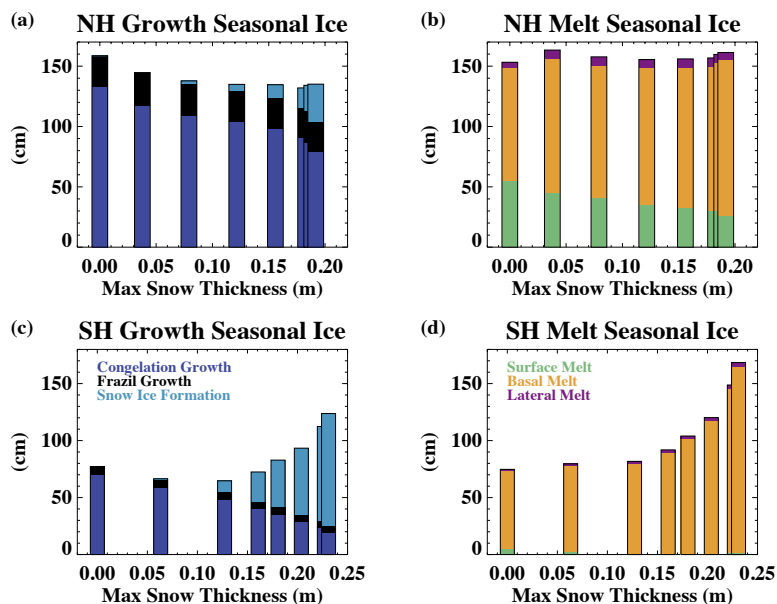

Figure 10. As in Figure 9 but for the seasonal sea ice region.

15

335

In the Southern Hemisphere (Figure 9c), congelation ice growth also dominates the growth sensitivity when snow depths are less than 0.2m. For deeper snow, increased snow-ice formation occurs, counteracting the decreasing congelation ice growth, and leading to a limited total growth sensitivity. Southern Hemisphere ice melt within the perennial ice zone (Figure 9d) shows very little sensitivity to snow. As indicated by the imbalance between melt and growth, most Southern Hemisphere ice within

340   the perennial zone is lost through transport to the seasonal ice zone. In the Arctic, perennial ice is also lost through transport to the seasonal ice zone but this plays a smaller role.

The net Northern Hemisphere seasonal ice growth (Figure 10a) is smaller than that of the perennial ice in all experiments because the seasonal ice occurs in a region of warmer ocean and atmospheric conditions. The seasonal ice growth declines

345   with increasing snow because of reduced congelation ice growth. The change in congelation growth per change in snow thickness computed from the end-member simulations (Fsnow=0 versus Fsnow=1.75) is considerably larger for the seasonal ice (2.8 cm growth per cm snow thickness) than for the perennial ice (1.5 cm growth per cm of snow thickness). This is consistent with thinner ice being more sensitive to the insulating effects of snow (Maykut, 1978). For the seasonal ice, the changes in congelation ice growth are largely compensated by increased snow ice formation for the thicker snow experiments

350   resulting in a limited sensitivity of the net growth to snow depth in those cases (Figure 10a). The Southern Hemisphere seasonal ice net growth (Figure 10c) is also smaller than that in the perennial ice zone (Figure 9c), again due to warmer ocean and air in the seasonal ice region. The seasonal ice has declining congelation growth and increasing snow-ice formation with thicker snow depths (Figure 10c). For simulations with thick snow cover, the snow-ice formation dominates and leads to overall increases in ice growth. By definition, all seasonal ice is melted away every year. In both hemispheres, basal melting dominates,

355   which is consistent with the influence of ocean heat availability in the seasonal ice zone.

The differences in the total hemispheric ice growth budgets in the two hemispheres (Figure 8) can be explained by differences in the relative importance of perennial and seasonal ice and the changing mass budgets within those regions. In the Northern Hemisphere, ice growth declines with increasing snow depths in both the seasonal and perennial ice packs as a consequence

360   of the insulating effect of the snow (Figure 9 and 10). However, the amount of seasonal ice also declines (Figure 11) and because that seasonal ice has reduced growth relative to the perennial ice, this counteracts the local insulating impact of the snow within each ice zone and causes a limited sensitivity of ice growth to snow depth for the hemispheric totals (Figure 8). In the Southern Hemisphere, the dominance of seasonal ice in all experiments (Figure 11) and increasing snow ice formation with snow depth (especially in the seasonal ice zone) results in an increase in growth with increasing snow depth on the
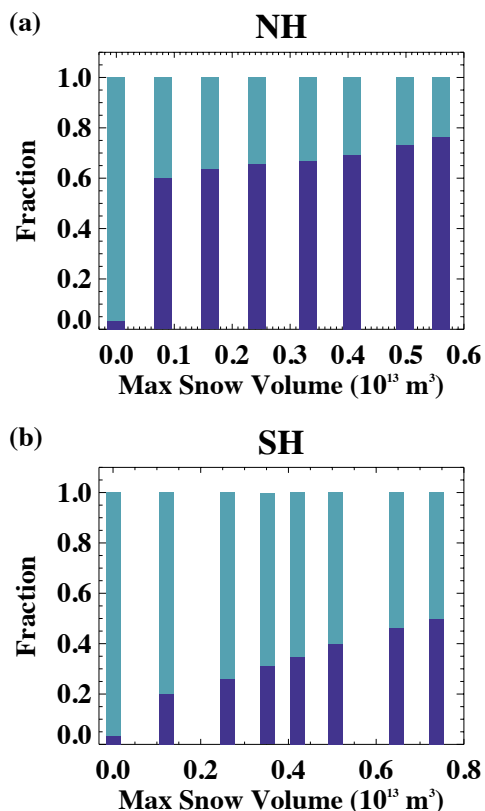
365   hemispheric scale.

(a)

(b)

Figure 11. The fraction of the total ice area occupied by seasonal ice (light blue) and perennial ice (dark blue) as a function of the maximum snow volume across the experiments. Values are shown for the (a) Northern Hemisphere and (b) Southern Hemisphere.

3.4 Response in a 2XCO2 Climate

The hemispheric differences in the sea ice response to changing snow cover are suggestive of a climate state dependence. In order to explicitly test how the influence of snow on sea ice may change in a changing climate, we have performed an additional set of simulations in a climate state with atmospheric CO_2 concentrations that are twice the preindustrial value (2XCO2 runs). We use the same experimental design where the snowfall on sea ice is multiplied by a constant factor (F_{snow}, see table 1). In the warmer 2XCO2 climate, more precipitation falls as rain and snowfall is reduced. Additionally, the area on which to accumulate snow is lower. These factors result in a smaller range of snow volume amounts across our sensitivity simulations. The Arctic is seasonally ice-free in all of the simulations performed and the Antarctic has considerable reductions in ice area compared to the pre-industrial runs.
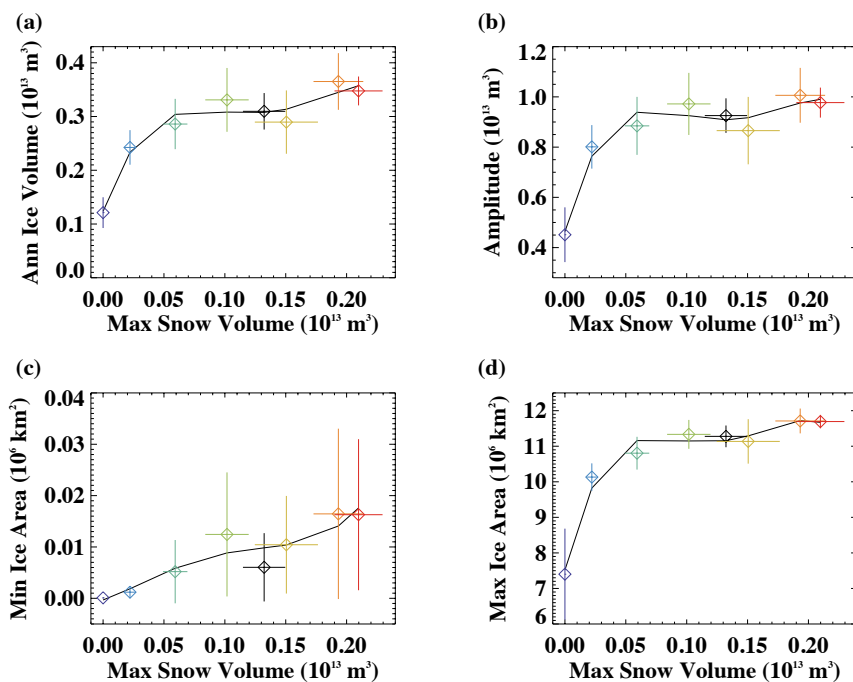
Figure 12. The relationship in the 2xCO2 simulations of the climatological Northern Hemisphere (a) annual ice volume, (b) amplitude of the ice volume annual cycle, (c) annual minimum ice area, and (d) annual maximum ice area versus the annual maximum snow volume. The diamonds show the simulated mean values and whiskers are +/- one standard deviation with the colors the same as in other figures. The black line is a 4th order polynomial fit.

The relationship between Northern Hemisphere sea ice properties and the maximum snow thickness is shown in Figure 12. With seasonal ice, higher air temperatures, and reduced snowfall present in the simulations, the snow accumulation is much reduced in the 2XCO2 climate, leading to a smaller variation in maximum snow volume across the simulations than in the preindustrial climate runs. Except for the no-snow case, the Northern Hemisphere ice volume, amplitude of the ice volume annual cycle, and minimum and maximum ice area are quite insensitive to the snow volume amount. The no-snow case does have significantly thinner ice, a lower amplitude annual cycle, and reduced maximum ice area. In the Southern Hemisphere (Figure 13), the ice volume, ice volume seasonal amplitude and ice area generally increase with increasing snow depths. This is quite similar to the results in preindustrial control simulations.
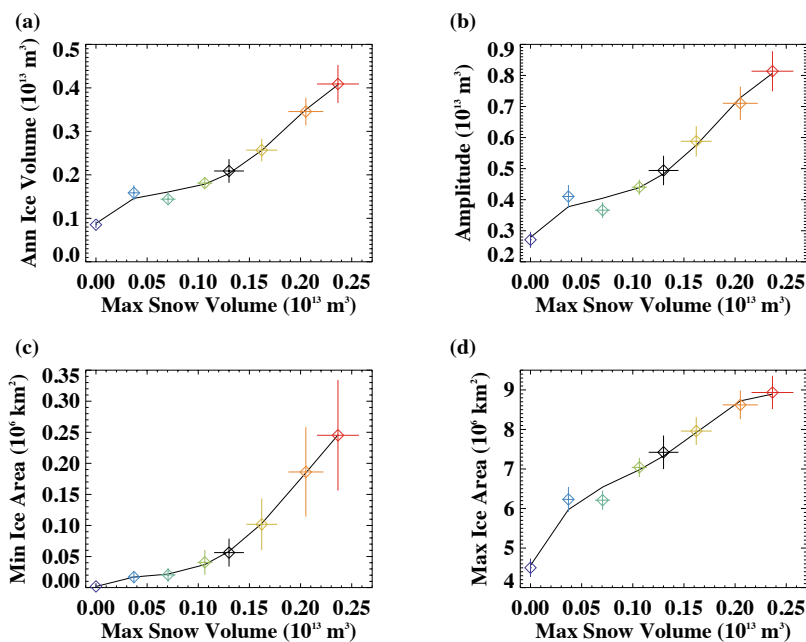
Figure 13. As in Figure 12 but for Southern Hemisphere values in the 2xCO2 climate.

The hemispheric mass budgets associated with the changing ice conditions in the simulated 2xCO2 climate are shown in Figure 14. In the Northern Hemisphere, congelation ice growth is smallest in the no-snow case and shows limited sensitivity to snow depth in the remaining simulations. The small growth sensitivity results from two largely compensating factors. With thicker snow, the insulating effect leads to reduced growth in the months when growth actually occurs. However, simulations with greater snow volume also have a lengthened ice growth season. This is a consequence of the albedo impact of the snow, which in the higher snow simulations contributes to later ice melt out, less summer ocean shortwave absorption and an earlier fall freezeup. These sensitivities are indicative of the Arctic in a completely seasonal ice regime. The Southern Hemisphere mass budgets in the 2xCO2 climate (Figure 14c and d) have a quite similar sensitivity to that of the preindustrial simulations, likely because of the prevalence of seasonal ice and snow-ice formation in both climate states. With increasing snow volumes, congelation ice growth declines but is more than compensated for by increases in snow-ice formation, leading to increased total ice growth. This is balanced primarily by increased basal melt.
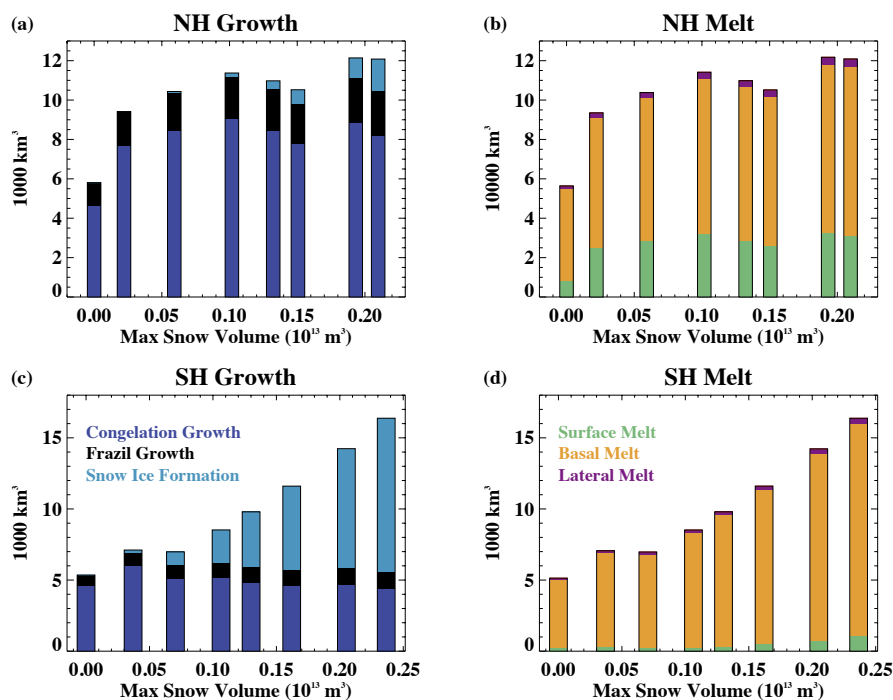
Figure 14. The volume in the 2xCO2 simulations of (a) Northern Hemisphere ice growth, (b) Northern Hemisphere ice melt, (c) Southern Hemisphere ice growth, and (d) Southern Hemisphere ice melt as a function of the maximum snow volume across the simulations.

4 Conclusions

We have performed CESM2 coupled climate model experiments in pre-industrial and 2xCO2 climate states with modified snowfall over sea ice. This has allowed us to isolate the influence of varying amounts of snow on sea ice in both hemispheres. In particular, we assess the influence on sea ice conditions and mass budgets. While previous studies have assessed the role of snow on sea ice, these have been done in the absence of coupled atmospheric feedbacks (e.g. Maykut and Untersteiner, 1971; Fichefet and Morales-Marqueda, 1999; Powell et al., 2005), for a perennial sea ice case (e.g. Maykut and Untersteiner, 1971), or for limited cases with simple models (Ledley, 1991). Our results do generally agree with these previous studies that increases in snow on sea ice result in a thicker ice cover and a cooler climate.

For the pre-industrial climate in the Northern Hemisphere, the ice volume, ice area, and fraction of perennial ice generally increase with increasing snow depths. These changes are non-linear with snow depth, consistent with previous studies (e.g. Maykut and Untersteiner, 1971). The Arctic atmosphere is colder with increased snow on sea ice, reinforcing the sea ice changes. Our simulations can be roughly categorized into the three regimes of no snow, seasonal snow, and perennial snow

cases. With no snow, the sea ice is thin, has a large annual cycle in ice volume, and is seasonally ice-free. In seasonal snow cases, with Fsnow from 0.25 to 1.25, the ice volume is relatively insensitive to snow depth, although the amplitude of the volume annual cycle does steadily decline. This suggests that for annual mean conditions, the insulating effect of the snow is

430   roughly balanced by the albedo influence. In the more perennial snow cases (Fsnow = 1.5 and 1.75), a considerable fraction of the ice remains snow covered year-round, and the ice is relatively thick. Increasing snow across the simulations results in a modest reduction in congelation ice growth and surface ice melt. However, the net hemispheric mass budgets are relatively insensitive to increasing snow. This is a consequence of the different mass budgets in seasonal and perennial ice zones and the changing perennial ice fraction across the simulations. With increasing snow, there is a significant reduction in growth of the

435   perennial ice (consistent for example with Maykut and Untersteiner, 1971) but also a growing perennial ice fraction. Because perennial ice is primarily located within the Arctic basin, it has higher growth rates than seasonal ice that occurs in the more southerly marginal ice zone in which warmer ocean and atmosphere conditions are present. As such, the increase in perennial ice fraction counteracts the reduction of perennial ice growth, leading to a limited snow-sensitivity for the hemispheric budgets.

440   In the Southern Hemisphere in a pre-industrial climate, the ice volume and area also increase with increasing snow depths. In contrast to the Northern Hemisphere, the ice volume annual cycle amplitude increases. With increasing snow, the Antarctic experiences more ice growth and more ice melt. This occurs because of the prevalence of snow-ice formation in the Antarctic, which is a consequence of relatively thin ice and high precipitation. With increased snow, snow-ice formation increases and overwhelms decreases in congelation ice growth that result from the snow insulating effect. The high ocean heat content in the

445   region allows this increased growth to be balanced by increased melting, which is almost entirely basal melt. The dominance of seasonal ice and high snow-ice formation result in a fundamentally different ice mass budget sensitivity to snow cover in the Southern Hemisphere as compared to the Arctic.

Differences in the climate conditions between the poles are largely responsible for the differing sea ice response to changing

450   snow amounts. This suggests that there may be a climate-state dependence to our results. In order to assess this, we performed experiments with varying snow amounts in a 2xCO2 climate. Except for the no-snow case, the Northern Hemisphere sea ice is quite insensitive to changing snow amounts. This may in part be due to the small range of snow accumulation that we are able to achieve with our experimental design because of the warm climate, low snowfall, and limited sea ice available as a platform to capture snowfall. All the 2xCO2 simulations have a seasonally ice-free Arctic and all (except for the no snow case)

455   have similar congelation ice growth, which is counter to what would be expected due to the insulating effect of the snowpack. This is likely in part associated with a larger influence of ice thickness on heat conductivity in the case of thin snow cover. Nevertheless, monthly values of congelation ice growth do decrease with greater snow but this is counteracted by a lengthened ice growth season leading to little sensitivity for the annual net growth. The longer ice growth season in simulations with more snow is in part a consequence of the higher surface albedo that leads to a later ice melt out, shortened ice-free season, and

460   reduced accumulation of solar heat in the ocean over the summer months.

In the Antarctic, while the ice is thinner and less extensive in the 2xCO2 run, the sensitivity to changing snow amounts is qualitatively similar to those in the pre-industrial climate state. In particular, with more snow, ice volume and area increase, and there is more ice growth as increases in snow-ice formation overwhelm decreases in congelation ice growth. We find little

465   evidence that Arctic sensitivity to snow on sea ice will resemble the Antarctic in a warming climate. However, in both hemispheres, although the reasons differ, we find that more snow is a "friend" to sea ice rather than a "foe", and results in increased ice volume and area and an overall cooler climate.

470   Author contribution: MMH, BL, and MS devised the experiments. MMH performed the experiments and analyzed the simulations. All authors contributed expertise on snow and sea ice processes. All authors contributed to the writing of the manuscript.

Competing Interests

475   The authors declare that they have no conflict of interest.

Code/data availability: The CESM2 model used for the experiments described here is publicly available for download from (https://www.cesm.ucar.edu/models/cesm2/release_download.html). Post-processed data from the experiments described here for the sea ice state, mass budgets, and polar atmosphere conditions will be made available through github upon acceptance of

480   the manuscript.

References

490   Andreas, E. L., and Ackley, S. F.: On the differences in ablation seasons of Arctic and Antarctic sea ice, J. Atmos. Sci., 389, 440-447, 1982.

Bacmeister J. T., Hannay C., Medeiros B., Gettelman A., Neale R., Fredriksen H. B., Lipscomb W. H., Simpson I., Bailey D. A., Holland M., Lindsay K., and Otto-Bliesner B.: CO2 increase experiments using the Community Earth System Model (CESM): Relationship to climate sensitivity and comparison of CESM1 to CESM2. *Journal of Advances in Modeling Earth Systems*, doi:10.1029/2020MS002120, 2020.

Bailey D. A., Holland M. M., DuVivier A. K., Hunke E. C., and Turner A. K: Impact of a New Sea Ice Thermodynamic Formulation in the CESM2 sea ice component. *Journal of Advances in Modeling Earth Systems*, doi:10.1029/2020MS002154, 2020.

Bintanja, R., and Selten, F.M.: Future increases in Arctic precipitation linked to local evaporation and sea-ice retreat. Nature **509**, 479–482, 2014.

Bitz, C. M. and Roe, G.H.: A Mechanism for the High Rate of Sea-Ice Thinning in the Arctic Ocean, J. Climate, 17, 3622—31, 2004.

Bitz, C.M, Holland, M.M., Hunke, E., and Moritz, R.E.: Maintenance of the sea-ice edge, *J. Climate*, 18, 2903-2921, 2005.

Bitz, C.M., Shell, K.M., Gent, P.R., Bailey, D., Danabasoglu, G., Armour, K.C., Holland, M.M., and Kiehl, J.T.: Climate sensitivity of the Community Climate System Model Version 4. *J. Climate*, 25, 3053-3070, doi:10.1175/JCLI-D-11-00290.1, 2012.

Blanchard-Wrigglesworth E, Armour, K.C., Bitz, C.M., and DeWeaver, E.: Persistence and inherent predictability of Arctic sea ice in a GCM ensemble and observations, *Journal of Climate*, 24, 231-250, doi: 10.1175/2010JCLI3775.1, 2011.

Blazey, B.A., Holland, M.M., and Hunke, E.C.: Arctic Ocean sea ice snow depth evaluation and bias sensitivity in CCSM., *The Cryosphere*, 7, 1887-1900, 2013.

Boisvert, L., Webster, M., Petty, A., Markus, T., Bromwich, D., and Cullather, R.: Intercomparison of precipitation estimates over the Arctic Ocean and its peripheral seas from reanalyses. Journal of Climate, 31(20), 8441–8462. doi:10.1175/JCLI-D-18-0125.1, 2018.

Brandt, R.E., Warren, S.G., Worby, A.P., and Grenfell, T.C.: Surface albedo of the Antarctic sea ice zone, Journal of Climate,
525 18, 3606-3622, 2005.

Briegleb, B. P., and Light, B.: A delta-Eddington multiple scattering parameterization for solar radiation in the sea ice
component of the Community Climate System Model. NCAR Tech. Note TN-4721STR, 100 pp, 2007.

530 Calonne, N., Flin, F., Morin, S., Lesaffre, B., Rolland du Roscoat, S., and Geindreau, C.: Numerical and experimental
investigations of the effective thermal conductivity of snow, Geophys. Res. Lett., 38, L23501, doi:10.1029/2011GL049234,
2011.

Danabasoglu, G., Lamarque, J. -F., Bachmeister, J., Bailey, D. A., DuVivier, A. K., Edwards, J., Emmons, L. K., Fasullo, J.,
535 Garcia, R., Gettelman, A., Hannay, C., Holland, M. M., Large, W. G., Lawrence, D. M., Lenaerts, J. T. M., Lindsay, K.,
Lipscomb, W. H., Mills, M. J., Neale, R., Oleson, K. W., Otto-Bliesner, B., Phillips, A. S., Sacks, W., Tilmes, S., van
Kampenhout, L., Vertenstein, M., Bertini, A., Dennis, J., Deser, C., Fischer, C., Fox-Kember, B., Kay, J. E., Kinnison, D.,
Kushner, P. J., Long, M. C., Mickelson, S., Moore, J. K., Nienhouse, E., Polvani, L., Rasch, P. J., and Strand, W. G: The
Community Earth System Model version 2 (CESM2). *Journal of Advances in Modeling Earth Systems*, 12
540 https://doi.org/10.1029/2019MS001916, 2019.

DeRepentigny, P., Jahn, A., Holland, M. M., and Smith, A: Arctic Sea Ice in Two Configurations of the Community Earth
System Model Version 2 (CESM2) During the 20th and 21st Centuries. *JGR: Oceans*, 125, e2020JC016133.
https://doi.org/10.1029/2020JC016133, 2020.

545

DuVivier, A. K., Holland, M. M., Kay, J. E., Tilmes, S., Gettelman, A., and Bailey, D. A: Arctic and Antarctic sea ice state
in the Community Earth System Model Version 2. *JGR: Oceans*, https://doi.org/10.1029/2019JC015934, 2020.

Fetterer, F., Knowles, K., Meier, W.N., Savoie, M., and Windnagel, A.K.: *Sea Ice Index, Version 3*. Boulder, Colorado USA.
NSIDC: National Snow and Ice Data Center. doi: https://doi.org/10.7265/N5K072F8. 2017.

550

Fichefet, T. and Morales-Marqueda, M.A.: Modelling the influence of snow accumulation and snow-ice formation on the
seasonal cycle of the Antarctic sea-ice cover, Climate Dynamics, 15, 251-268, 1999.

Gettelman, A., Hannay, C., Bacmeister, J. T., Neale, R. B., Pendergrass, A. G., Danabasoglu, G., et al.: High climate sensitivity
555 in the Community Earth System Model Version 2 (CESM2). Geophysical Research Letters, 46, 8329– 8337.
https://doi.org/10.1029/2019GL083978, 2019.

Gordon, A. L.: Seasonality of Southern Ocean sea ice, J. Geophys. Res., 86(C5), 4193-4197, 1981.

560   Hezel, P.J., Zhang, X., BItz, C.M., Kelly, B.P., and Massonnet, F.: Projected decline in spring snow depth on Arctic sea ice caused by progressively later autumn open ocean freeze-up this century, Geophys. Res. Lett., https://doi.org/10.1029/2012GL052794, 2012.

Holland, M.M. and Landrum, L.: Factors affecting projected Arctic surface shortwave heating and albedo change in coupled
565   climate models, *Phil. Trans. R. Soc. A*, 373:20140162, doi:10.1098/rsta.2014.0162, 2015.

Holland, M.M., Bailey, D.A., Briegleb, B.P., Light, B., and Hunke, E.: Improved sea ice shortwave radiation physics in CCSM4: The impact of melt ponds and black carbon. *J. Climate*, 25 (5), 1413-1430. doi:10.1175/JCLI-D-11-00078.1, 2012.

570   Hunke, E. C., and Dukowicz, J.K.: The elastic–viscous–plastic sea ice dynamics model in general orthogonal curvilinear coordinates on a sphere—Incorporation of metric terms. Mon. Wea. Rev., 130, 1848–1865, 2002.

Hunke, E. C.*, Lipscomb, W. H.*, Turner, A. K.*, Jeffery, N.*, and Elliott, S.*: CICE: The Los Alamos Sea Ice Model Documentation and Software User's Manual Version 5.1 LA-CC-012. *Retrieved from* https://github.com/CICE-
575   Consortium/CICE-svn-trunk/blob/master/cicedoc/cicedoc.pdf, 2015.

Kacimi, S. and R. Kwok, R.: The Antarctic sea ice cover from ICESat-2 and CryoSat-2: freeboard, snow depth, and ice thickness, The Cryosphere, 14, 4453-4474, https://doi.org/10.5194/tc-14-4453-2020, 2020.

580   Kattsov, V. M., Walsh, J.E., Chapman, W.L., Govorkova, V. A., Pavlova, T. V. and Zhang, X.D.: Simulation and projection of arctic freshwater budget components by the IPCC AR4 global climate models, J. Hydrometeorol., 8, 571–589, 2007.
Labe, Z., Madnusdottir, G., and Stern, H.: Variability of Arctic sea ice thickness using PIOMAS and the CESM Large Ensemble, J. Climate, 31, 3233-3247, doi:10.1175/JCLI-D-17-0436.1, 2018.

585   Lawrence, D.M., Fisher, R.A., Koven, C.D., Oleson, K.W., Swenson, S.C., Bonan, G., Collier, N., Ghimire, B., van Kampenhout, L., Kennedy, D., Kluzek, E., Lawrence, P.J., Li, F., Li, H., Lombardozzi, D., Riley, W.J., Sacks, W.J., Shi, M., Vertenstein, M, Wieder, W.R., Xu, C., Ali, A.A, Badger, A.M., Bisht, G., van den Broeke, M., Brunke, M.A., Burns, S.P., Buzan, J., Clark, M., Craig, A., Dahlin, K., Drewniak, B., Fisher, J.B., Flanner, M., Fox, A.M., Gentine, P., Hoffman, F., Keppel-Aleks, G., Knox, R., Kumar, S., Lenaerts, J., Leung, L.R., Lipscomb, W.H., Lu, Y., Pandey, A., Pelletier, J.D., Perket,,
590   J., Randerson, J.T., Ricciuto, J.M., Sanderson, B.M., Slater, A., Subin, Z.M., Tang, J., Thomas, R.Q., Val Martin, M., and

Zeng, X.: The Community Land Model version 5: Description of new features, benchmarking, and impact of forcing uncertainty. *Journal of Advances in Modeling Earth Systems*, 11. https://doi.org/10.1029/2018MS001583, 2019.

595 Ledley, T. S.: Snow on sea ice: Competing effects in shaping climate, J. Geophys. Res., 96(D9), 17,195–17,208, 1991.

Leonard, K.C. and Maksym, T.: The important of wind-blown snow redistribution to snow accumulation on Bellingshausen Sea ice, Annals of Glaciology, 52 (57), 271-278, doi:10.3189/172756411785831651, 2011.

600 Maksym, T., and Jeffries, M.O.: A one-dimensional percolation model of flooding and snow ice formation with particular reference to sea ice in the Ross Sea, Antarctica, J. Geophys. Res., 105(C11), 26,313–26,331, 2000.

Massom, R.A., Eicken, H., Haas, C., Jeffries, M.O., Drinkwater, M.R., Sturm, M., Worby, A.P., Wu, X., Lytle, V.I., Ushio, S., Morris, K., Reid, P.A., Warren, S.G., and Allison, I.: Snow on Antarctic sea ice. Reviews of Geophysics, 39 (3), 413-445,
605 2001.

Maykut, G.A., Energy exchange over young sea ice in the central Arctic, J. Geophys. Res., 83 (C7), 3646-3658, 1978.

Maykut, G. A., and Untersteiner, N.: Some results from a time-dependent thermodynamic model of sea ice, J. Geophys. Res.,
610 76(6), 1550–1575, 1971.

Perket, J., Flanner, M.G., and Kay, J.E.: Diagnosing shortwave cryosphere radiative effect and its 21st century evolution in CESM, JGR Atmospheres, https://doi.org/10.1002/2013JD021139, 2014.

615 Perovich, D. K., Grenfell, T. C., Light, B. and Hobbs., P. V.: Seasonal evolution of the albedo of multiyear Arctic sea ice. J. Geophys. Res. 107(C10), 8044, 2002.

Petty, A.A., Holland, M.M., Bailey, D.A., and Kurtz, N.T.: Warm Arctic, increased winter sea-ice growth? *Geophys. Res. Lett.*, doi:10.1029/2018GL079223, 2018.
620

Powell, D.C., Markus, T., and Stossel, A.: Effects of snow depth forcing on Southern Ocean sea ice simulations, JGR Oceans, https://doi.org/10.1029/2003JC002212, 2005.

Raphael, M. N., Handcock, M. S., Holland, M. M., and Landrum L. L.: An assessment of the temporal variability in the
625 annual cycle of daily Antarctic sea ice in the NCAR Community Earth System Model, Version 2: A comparison of the
historical runs with observations. *JGR: Oceans*, doi:10.1029/2020JC016459, 2020.

Schweiger, A., Lindsay, R., Zhang, J., Steele, M., Stern, H., and Kwok, R.: Uncertainty in modeled Arctic sea ice volume. J.
Geophys. Res., 116, C00D06, doi:10.1029/2011JC007084, 2011.
630
Semtner, A. J.: A Model for the Thermodynamic Growth of Sea Ice in Numerical Investigations of Climate. J Phys Oceanogr,
6, 379-389, 1976.

Singh H. K. A., Landrum L., Holland M. M., Bailey, D.A., and DuVivier, A.K.: An Overview of Antarctic Sea Ice in
635 CESM2 Part I: : Analysis of the Seasonal Cycle in the context of sea ice thermodynamics and coupled atmosphere-ocean-ice
processes. *Journal of Advances in Modeling Earth Systems*, doi:10.1029/2020MS002143, 2020.

Stroeve, J.C., Markus, T., Boisvert, L., Miller, J., and Barrett, A.: Changes in Arctic melt season and implications for sea ice
loss, Geophysical Res. Lett., 41(4), 1216-1225, https://doi.org/10.1002/2013GL058951, 2014.
640
Stroeve, J.C., Schroder, D., Tsamados, M., and Feltham, D.: Warm winter, thin ice? The Crysophere, 12(5), 1791-1809.
https://doi.org/10.5194/tc-12/1791-2018, 2018.

Sturm, M., Holmgren, J., König, M., and Morris, K.: The thermal conductivity of seasonal snow, J. Glaciol., 43(143), 26–41,
645 1997.

Sturm, M. & Massom, R. A. in Sea Ice 3rd edition (ed. Thomas, D. N.) 65–109, Wiley and Blackwell, Oxford, 2017.

Sturm, M., Perovich, D. K. and Holmgren, J.: Thermal conductivity and heat transfer through the snow on the ice of the
650 Beaufort Sea. J. Geophys. Res. 107(C21), 8043, 2002.

Turner, A. K., and Hunke, E.C.: Impacts of a mushy-layer thermodynamic approach in global sea-ice simulations using the
CICE sea-ice model. J. Geophys. Res. Oceans, 120, 1253–1275, doi:10.1002/2014JC010358, 2015.

655 Vihma, T., Screen, J., Tjernstrom, M., Newton, B., Zhang, X., Popova, V., Deser, C., Holland, M., and Prowse, T.: The atmospheric role in the Arctic water cycle: processes, past and future change, and their impacts, *J. Geophys. Res.-Biogeosci.*, 121, doi:10.1002/2015JG003132, 2015.

Webster, M. A. et al. Interdecadal changes in snow depth on Arctic sea ice. J. Geophys. Res. Oceans 119, 5395–5406, 2014.
660

Webster M. A., DuVivier A. K., Holland M. M., and Bailey D. A.: Snow on Arctic sea ice in a warming climate as simulated in CESM2. *Journal of Advances in Modeling Earth Systems,* https://doi.org/10.1029/2020JC016308, 2020.

Webster, M., Gerland, S., Holland, M., Hunke, E., Kwok, R., Lecomte, O., Massom, R., Perovich, D., and Sturm, M.: Snow
665 in the changing sea ice systems. *Nature Climate Change*, doi:10.1038/s41558-018-0286-7, 2018.

Worby, A.P., Geiger, C.A., Paget, M.J., Van Woert, M.L., Ackley, S.F., and DeLiberty, T.L.: Thickness distribution of Antarctic sea ice, J. Geophys. Res.-Oceans, 113(C5),
https://doi.org/10.1029/2007JC004254, 2008.
670

Zhang, R., Wang, H., Fu, Q., Rasch, P.J., and Wang, X.: Unraveling driving forces explaining significant reduction in satellite-inferred Arctic surface albedo since the 1980s, PNAS, 116 (48) 23947-23953, https://doi.org/10.1073/pnas.1915258116, 2019.